

## Original Research Article

# Green synthesis of copper oxide nanoparticles using *Abutilon indicum* leaf extract: Antimicrobial, antioxidant and photocatalytic dye degradation activities

Faheem Ijaz<sup>1</sup>, Sammia Shahid<sup>1</sup>, Shakeel Ahmad Khan<sup>1\*</sup>, Waqar Ahmad<sup>1</sup>, Sabah Zaman<sup>2</sup>

<sup>1</sup>Department of Chemistry, School of Science, University of Management & Technology, Lahore-54770, <sup>2</sup>Ibn-e-Sina Institute of Technology, Islamabad-44000, Pakistan

\*For correspondence: **Email:** [Shakilahmad56@gmail.com](mailto:Shakilahmad56@gmail.com); **Tel:** +92-3441865064

Received: 6 December 2016

Revised accepted: 20 March 2017

### Abstract

**Purpose:** To synthesize copper oxide (CuO) nanoparticles using a ecofriendly technique and evaluate their antimicrobial, antioxidant and photo-catalytic dye degradation potentials.

**Methods:** A superficial method (solution combustion method) was employed for the synthesis of copper oxide nanoparticles from an aqueous extract of *Abutilon indicum*. The CuO nanoparticles were characterized using x-ray diffraction (XRD), energy-dispersive x-ray spectroscopy (EDX), scanning electron microscope (SEM) and ultraviolet-visible (UV-Vis) spectroscopic techniques. The antimicrobial activity of the CuO nanoparticles was determined by agar well diffusion method, while their antioxidant properties were assessed by DPPH radical scavenging, ferric reducing antioxidant power (FRAP), total antioxidant, ferric thiocyanate (FTC) and total phenolic content (TPC) assays. The photo-catalytic degradation activity of synthesized CuO nanoparticles was assessed by the degradation of Acid Black 210 (AB) dye under sunlight irradiation.

**Results:** XRD, EDX and SEM results confirmed successful synthesis of CuO nanoparticles, with hexagonal, wurtzite and sponge crystal structure. Photo-catalytic data revealed that the nanoparticles are a good catalyst for effective degradation of Acid Black 210. The nanoparticles also exhibited remarkable antioxidant activity, with  $IC_{50}$  and FRAP values ranging from  $40 \pm 0.23$  to  $84 \pm 0.32$   $\mu\text{g/ml}$ , and  $0.65 \pm 0.01$  to  $9.10 \pm 0.21$  Trolox equivalent/mL, respectively. Significant bactericidal activity was manifested by the CuO nanoparticles against *Klebsiella* and *Bacillus subtilis* with zone of inhibition of  $14 \pm 0.05$  and  $15 \pm 0.11$  mm, respectively.

**Conclusion:** The synthesized CuO nanoparticles exhibit antibacterial and antioxidant potential, indicating that they are good candidates for future therapeutic applications.

**Keywords:** CuO nanoparticles, Green synthesis, Photo-catalytic degradation, Antioxidant, Antimicrobial

Tropical Journal of Pharmaceutical Research is indexed by Science Citation Index (SciSearch), Scopus, International Pharmaceutical Abstract, Chemical Abstracts, Embase, Index Copernicus, EBSCO, African Index Medicus, JournalSeek, Journal Citation Reports/Science Edition, Directory of Open Access Journals (DOAJ), African Journal Online, Bioline International, Open-J-Gate and Pharmacy Abstracts

## INTRODUCTION

Copper oxide (CuO) has a wide range of applications in various fields, from energy conversion and storage through environmental science, electronics and sensor [1]. CuO nanoparticles have received a lot of attention

because they are the simplest members of the family of copper salts, and they possess a range of useful physical properties such as electron correlation effects, spin dynamics and high temperature superconductivity [2]. The unique properties of CuO nanoparticles and their potential applications have continued to attract a

lot of attention [3]. CuO nanoparticles are used to improve viscosity of energy transferring fluids, thereby boosting thermal conductivity [4]. In industrial fields, CuO nanoparticles are widely used as p-type semiconductors and transistors in the design and production of batteries [4], solar cells [5], gas sensors [6] and field emitters [7]. Nowadays, CuO nanoparticles are utilized as heterogeneous catalysts [7], antioxidants, drug delivery agents, and imaging agents in field of biomedicine [1-3].

Data related to antimicrobial activity of CuO nanoparticles is very limited [4,5]. These nanoparticles are robust and stable, and their shelf life is longer when compared with organic antimicrobial agents [2]. Copper oxide is less expensive when compared to silver and gold which possess antimicrobial potential. CuO nanoparticles are potentially highly valuable antimicrobial agents due to the fact that when synthesized, they possess extremely unusual crystal morphologies and high surface areas [5]. The use of plant extracts for the synthesis of nanoparticles is a gradually-evolving research area known as green synthesis of nanoparticles (NPs) [6]. In green synthesis of metal nanoparticles, the difficult task is to find a suitable and non-toxic natural product, as well as an eco-friendly solvent system [7]. Recently, material scientists have focused on green routes for the synthesis and production of nanoparticles [2].

*Abutilon indicum* is an erect, woody and shrubby plant that belongs to the *Malvaceae* family. This plant which is widely distributed in Pakistan is locally known as *peelybooti* or *karandi*.

The current study was aimed at green synthesis of CuO nanoparticles using aqueous leaf extract of *Abutilon indicum* as a green fuel, and determination of the antioxidant and antimicrobial properties of the synthesized nanoparticles.

## EXPERIMENTAL

This research work was carried out in the Research Laboratory of Department of Chemistry, University of Management and Technology, Lahore Pakistan, and in Research and Development Laboratory in Shafi Reso-Chem, Lahore Pakistan. All chemicals used were of analytical grade; and were purchased from Merck and Sigma-Aldrich. These included butylated hydroxytoluene, BHT (99.0 %); 2, 2-diphenyl-1-picrylhydrazyl radical DPPH (90.0 %); Folin-ciocalteu reagent (2N), linoleic acid and catechin.

## Collection of plants materials

Fresh leaves of *Abutilon indicum* were collected from Christian graveyard, Jallo, near Ring Road Interchange, Barki, and District Lahore, Pakistan in May 10, 2016. The leaves were identified and authenticated by a taxonomist, Dr. Ghazala Yasmeen Butt, of Botany Department, GC University Lahore, Pakistan in May 12, 2016. A voucher specimen was submitted to the herbarium of GC University Lahore, Pakistan for future reference (Voucher number: GC-HERB-564).

## Sample and extract preparation

The fresh leaves of *Abutilon indicum* were washed gently to remove dust particles and dried in a shaded place at room temperature (22 - 25 °C). Thereafter, the leaves were pulverized using a commercial blender (TSK-949, West point, France), and sieved in a 200 mesh sieve (0.074 mm diameter particle size). The plant material powder was placed in a Soxhlet apparatus for continual solvent extractions. Water was employed as a solvent for the extraction. The temperature of the apparatus was set at 90-95 °C and the extraction lasted for approximately 3 h. The resultant extract was filtered using sintered glass crucible, and then concentrated under vacuum in a rotary flash evaporator (vacuum was created by using 1/3HP 4 CFM Rotary Vane Deep Vacuum Pump HVAC Tool for AC R410a R134). The concentrated extract was then dried over a water bath, and the crude plant extract was taken in an air-tight bottle and stored in refrigerator.

## Synthesis of nanoparticles

CuO nanoparticles were synthesized using the green combustion method, with the leaf extract of *Abutilon indicum* as fuel. Copper (II) nitrate trihydrate { $\text{Cu}(\text{NO}_3)_2 \cdot 3\text{H}_2\text{O}$ , 1.205 g} was mixed with 0.3 g *Abutilon indicum* extract in 20ml of double-distilled water. The solution was homogenized for 2-5 min with constant stirring using a magnetic stirrer at the rate of 2000 rpm. Before starting the combustion process, the muffle furnace was heated to  $400 \pm 5$  °C. Thereafter, the sample was taken in clay crucible and then placed in the pre-heated muffle furnace at temperature  $400 \pm 5$  °C (with the aid of a long iron sample holder). Combustion of the mixture was completed within 2 - 3 min., resulting in production of CuO nanoparticle as presented in Figure 1. The resultant mixture was filtered to remove the ash contents of the plant extracts. The solution was washed with distilled water, followed by methanol to remove impurities.

Furthermore, the synthesized CuO nanoparticles were calcinated for 2 h to attain purity. This yielded fine, black CuO nanoparticles which were stored in an airtight container.

### Characterization of nanoparticles

Energy dispersive x-ray technique was employed for determination of the composition of the synthesized CuO nanoparticles. In addition, characterization of crystallite structure of the CuO nanoparticles was done using the XRD i.e. PANalytical X'Pert diffractometer instrument with Cu-K $\alpha$  radiation (wavelength, 0.154 nm) operating at 40 kV and 30 mA. Measurements were scanned for diffraction angles ( $2\theta$ ) ranging from  $20^\circ$  to  $90^\circ$  with a step size of  $0.02^\circ$  and a time per step of 1 s. The absorption spectrum and band gap energies of the CuO nanoparticles were analyzed by UV-visible spectrophotometer (Spectra Flash SF 550, Data color Inc., USA). Their morphological features were determined using SEM (Jeol, 5910LV).

### Photo-catalytic degradation activity

Photo-catalytic degradation activity of the CuO nanoparticles was estimated by the disintegration of Acid Black 210 (AB) dye under sunlight irradiation. For this assay, 0.005 g of synthesized CuO nanoparticles was dispersed in 5 mL distilled water in a test tube and then ultrasonicated. Ten milliliters of 13 mM Acid Black 210 dye solution was added to 5 mL of the CuO nanoparticle solution, and kept in the dark for 30 min. To obtain adsorption-desorption stage, the CuO nanoparticle suspension with Acid Black 210 was exposed at different time intervals (20, 40, and 60 min). This experiment was performed between 11 am to 1 pm. The suspensions obtained were centrifuged for two min, and the concentration of Acid Black 210 in the resultant solution was monitored in the

wavelength range of 200 - 800 nm in a UV-visible spectrophotometer. Distilled water was used as reference.

### DPPH free radical scavenging assay

The known antioxidant value of BHT was compared with unknown values of given sample of 2, 2-diphenyl-1-picrylhydrazyl according to the method of Khan *et al*, [9]. Three milliliters of a solution of DPPH (0.1mM) in methanol was mixed with different concentrations of the sample. Each solution mixture was continuously mixed for ten minutes at room temperature i.e. at  $22-25^\circ\text{C}$  to attain homogeneity, and then allowed to stand for 1 hr. The absorbance of given solution was measured in a spectrophotometer at 517 nm against methanol as blank. Antioxidant activity (D) was determined as in Eq 1.

$$D (\%) = \{(A_c - A_s)/A_c\}100 \dots\dots\dots (1)$$

where  $A_s$  and  $A_c$  are the absorbance of sample and control, respectively.

### Total antioxidant assay (TAA)

The antioxidant potential of the CuO nanoparticles was evaluated by determining total antioxidant activity according to the procedure described by Prieto *et al*, [10]. CuO nanoparticles (0.5 mg/mL) and 4 mL of reagent solution (28 mM sodium phosphate, 4 mM ammonium molybdate and 0.6 M sulphuric acid,) were put in a capped test tube and incubated in a water bath at  $95^\circ\text{C}$  for 90 min. The incubated sample was thereafter cooled to room temperature and the absorbance was measured at 695 nm against blank. Antioxidant activity was expressed relative to that of BHT which was used as standard. All assays were carried out in triplicate.

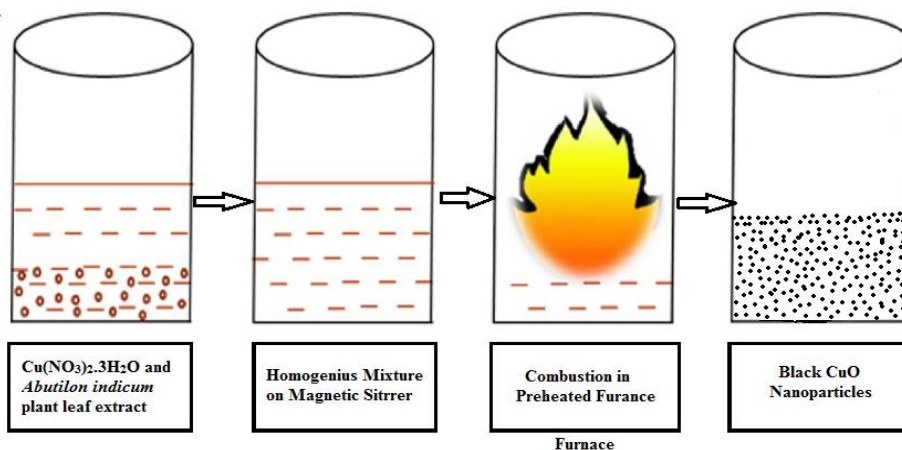


**Figure 1:** Illustration of the synthesis of CuO nanoparticles

### Ferric reducing antioxidant power (FRAP) assay

This was done by the method of Benzie *et al* [11]. A stock solution was prepared by mixing 10 mM TPTZ (2,4,6-tripyridyl-s-triazine), 300 mM acetate buffer (3.1 g sodium acetate trihydrate and 16 mL acetic acid, pH 3.6) and 20 mM ferric chloride hexahydrate in 40 mM HCl. Prior to use, a working solution was prepared by mixing 25 mL of acetate buffer, and 2.5 mL of TPTZ solution in 2.5 mL ferric chloride hexahydrate, and warming at 37 °C. Trolox and sample solutions were prepared in methanol (1mg/mL). Each sample (10 µL) and BHT solution were taken in separate test tubes and 2.99 mL of FRAP solution were added to make the total volume up to 3 mL. The FRAP solution was mixed with sample and reaction was allowed to take place for 30 min in the dark. Absorbance readings were determined for the colored product (ferrous tripyridyltriazine complex) at 593 nm. Corresponding FRAP values were expressed as micromole of Trolox equivalent (TE) per mL of sample by extrapolation from a standard calibration curve constructed with different concentrations of Trolox. Results were expressed as µmole TE /mL.

### Total phenolic content (TPC) assay

The total phenolic content of the CuO nanoparticles was determined by the colorimetric method of Makkar *et al*, [12]. A fresh solution was prepared by dissolving 0.5 mg of the nanoparticles in 1 mL of distilled water. This solution (0.1 mL) was added to 0.1 mL of 2N Folin-Ciocalteu reagent and 2.8 mL of 10 % Na<sub>2</sub>CO<sub>3</sub>. The mixture was shaken and allowed to stand for 40min, and absorbance was read at 725 nm in a UV-visible spectrophotometer. Total phenolics were extrapolated from a gallic acid standard calibration curve, and expressed as micrograms of gallic acid equivalents (GAE) per mL (µg GAE/mL). The standard curve was linear between 0.05 to 0.4 mg/mL of gallic acid.

### Ferric thiocyanate (FTC) assay

The inhibitory effect of the sample on linoleic acid peroxidation was studied by using the thiocyanate method of Valentao *et al* [13]. The reaction mixture contained linoleic acid emulsion (2.5 mL, 0.02 M, pH 7); 2.0 mL of phosphate buffer (0.02 M, pH 7) and 0.1 mL of sample solution (0.5 mg/mL) (the linoleic acid emulsion was prepared by mixing 0.28 g of linoleic acid, 0.28 g of Tween-20 as emulsifier, and 50.0 mL of phosphate buffer). This reaction mixture was heated in an incubator at 40 °C for 5 days. A

mixture without sample was used as blank. At the end of the reaction, 0.5 mL of reaction mixture was added to 5 mL of 75 % alcohol, 0.5 mL of 30 % ammonium thiocyanate and 0.1 mL of 20 mM ferrous chloride (in 3.5 % HCl), and mixed. The solution was allowed to stand for about three minutes at room temperature, and absorbance was read at 592 nm. The antioxidant activity was expressed as inhibition of peroxidation (IP %) computed as in Eq 2.

$$IP (\%) = \{1 - (As/(Ac))\}100 \dots\dots\dots (2)$$

where As and Ac are the absorbance of test sample and control, respectively.

### Evaluation of antimicrobial activity

The antimicrobial activity of the synthesized CuO nanoparticles was determined by using the Agar well diffusion method of Khan *et al*, [14]. The bacteria used for the antibacterial activity were *E. coli*, *B. subtilis*, *Staphylococcus aureus* and *Klebsiella*. *E. coli* represented Gram-negative bacteria while *B. subtilis*, *Staphylococcus aureus*, and *Klebsiella* represented Gram-positive bacteria. For positive control, bacteriological ampicillin was used as standard antibiotic while distilled water was used as negative control of all the species. Ultrasonication method was used for preparation of solution of the CuO nanoparticles in distilled water. Two different concentrations of nanoparticle solutions were prepared, i.e., 3 mg and 5 mg. For the reference antibiotic, 1 mg was used in the present study.

## RESULTS

### Characteristics of nanoparticles

The morphological and structural properties of the CuO nanoparticles were observed using SEM. The resultant images are shown in Figure 2. The synthesized nanoparticles had sizes which are in the nanometer range and their structures were not homogenous. These images indicate that only few nanoparticles with spherical shape were synthesized. Some nanoparticles were well separated from each other while most were present in agglomerated form. Thus, these SEM results confirmed the nanostructure behavior of the synthesized particles. The results are in agreement with previous reports [3,15] although with some slight differences due to chemical composition.

### Energy dispersive x-ray spectra

EDX studies were carried out in order to confirm presence of CuO nanoparticles and also to

examine the chemical formation and composition of the prepared sample. The EDX spectra are shown in Figure 3. It confirms the presence of all constituent elements, i.e., copper (Cu), oxygen (O), sulphur (S), phosphorus (P) and silicon (Si) in the CuO nanoparticles synthesized. The constituent elements are represented in Table 1. The EDX spectra also confirmed the presence CuO in the prepared sample. It is clear from Figure 3 that the EDX pattern confirmed successful formation of CuO nanoparticles with the leaf extract of *Abutilon indicum*. The EDX peak positions were consistent with copper

oxide, and the sharp peaks of EDX indicated that the synthesized CuO nanoparticles had crystalline structure. The other peaks observed in the EDX spectrum were due to impurities from Si, P and S which were present in the substrate. The strong intensity and narrow width of CuO diffraction peaks indicate that the resultant products were highly crystalline in nature. Hence we can conclude that the green fuel played profound role in controlling particle size. These findings are in close agreement with previous reports [16] but with slight difference due to variations in chemical composition.

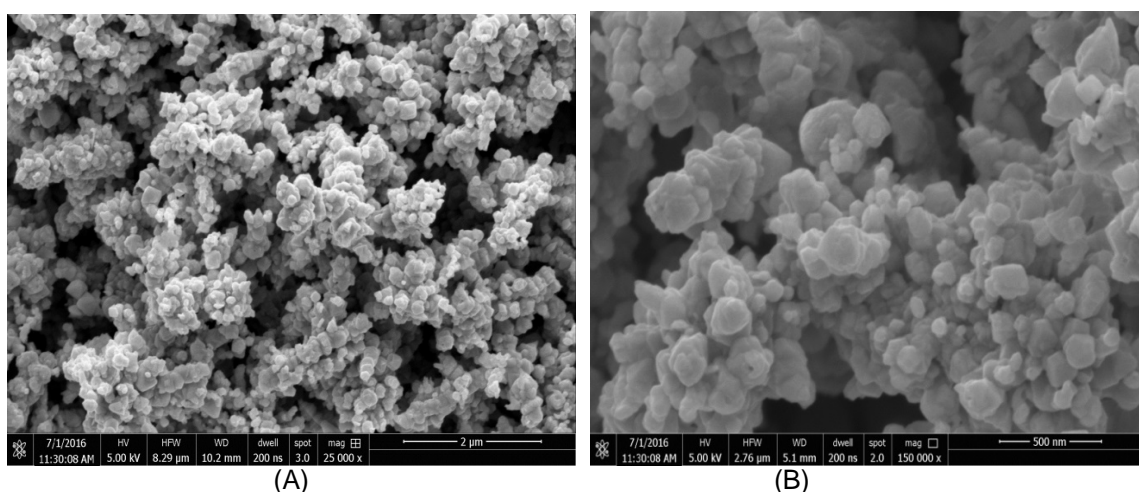


**Figure 2:** (A) SEM image of CuO nanoparticles taken at 2  $\mu\text{m}$ , (B) SEM image of CuO nanoparticles taken at 500  $\mu\text{m}$

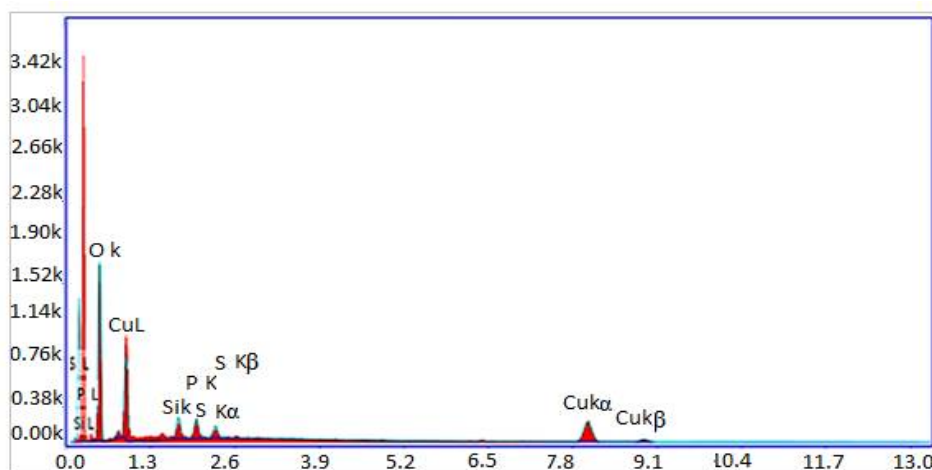


**Figure 3:** EDX spectra of copper oxide nanoparticles

**Table 1:** Constituent elements and their percentage values

Element	Atomic (%)	Weight (%)	Net Int.	Error (%)
O K	52.09	77.5	264	7.64
Si K	3.8	3.22	36.89	13.45
P k	4.52	3.47	41.31	13.09
S k	2.64	1.96	27.02	15.78
Cu K	36.95	13.84	90.14	5.11

### X-ray diffraction

Figure 4 shows the XRD pattern of CuO nanoparticles. The sharp diffraction peaks in the XRD pattern distinctly depict the crystalline nature of the sample [1,2]. The standard diffraction peaks representing the crystal structure of CuO is hexagonal wurtzite structure according to the standard JCPDS data card. Diffraction peaks of other impurities were not detected. This proved that the peaks which were observed in the XRD spectrum belonged only to the Cu.

The mean grain size of the CuO nanoparticles was 16.78 nm. This was calculated from the three most intense peaks using Debye-Scherrer's formula [2,3].

### Band gap energy

The band gap of the CuO nanoparticles was obtained by plotting absorptivity  $(\alpha h\nu)^2$  as a

function of energy (h $\nu$ ). Extrapolating the linear portion of the curve to absorption axis gives the band gap energies of CuO nanoparticles which were 3.378 eV. This band gap energy value for CuO nanoparticles is in close proximity to previously reported data, although slightly higher. This slightly higher value of energy band gap for CuO nanoparticles was due to the energy band gap confinement effect [17]. Energy band gap data for CuO Naps is presented in Figure 5.

### Photo-catalytic dye degradation

Disintegration of organic dye by the CuO nanoparticles is shown in Figure 6 and in Figure 7 with slight modification as presented by Lai *et al* [18]. In the first step, cupric oxide nanostructure comes in contact with light, creating a photo-generated electron and a hole. The photo-generated electron reacts with oxygen molecule to form superoxide free radical in the second step.

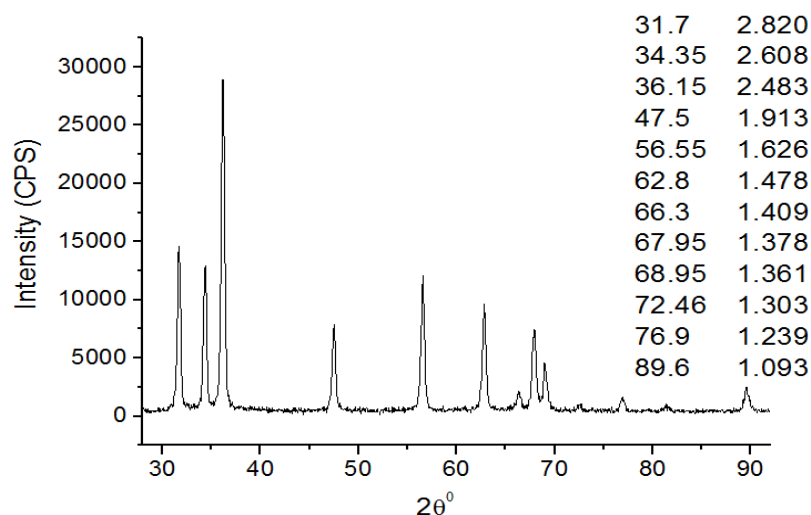


**Figure 4:** XRD spectrum of synthesized CuO nanoparticles

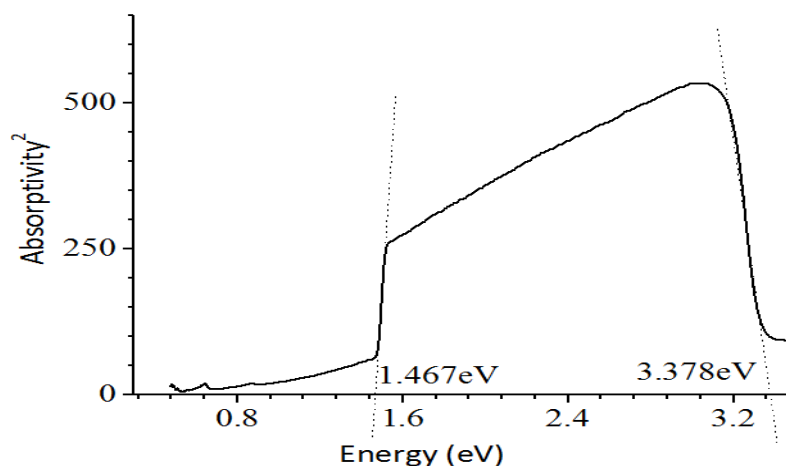


**Figure 5:** Band Gap Energy graph of the synthesized CuO nanoparticles

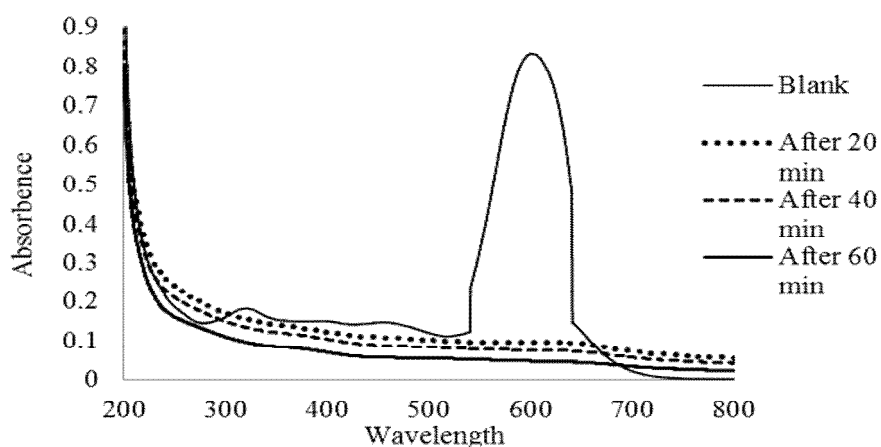


Figure 6: Photo-catalytic activity of synthesized CuO nanoparticles

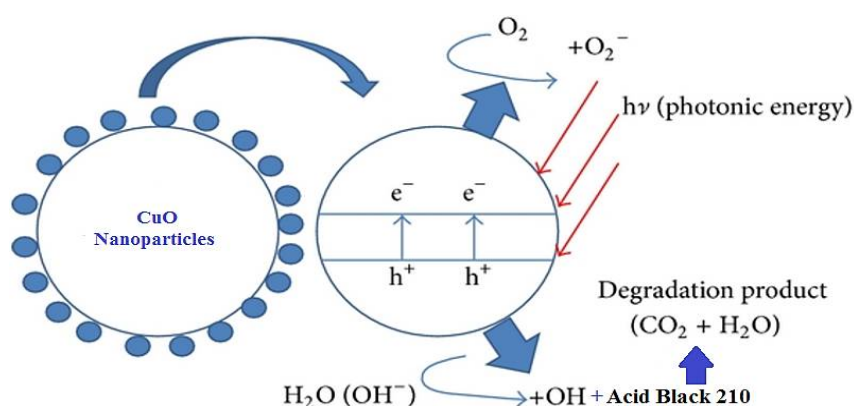


Figure 7: Photocatalytic activity of synthesized CuO nanoparticles [18]

In the third step, the hole reacts with water and hydroxyl ions to produce highly mercurial hydroxyl radicals. These superoxide free radicals and hydroxyl free radicals react violently with Acid Black 210 organic dye and decompose/decolorize it in the next step. The degradation/decomposition rate of the organic dye totally depends on morphological and crystal structure of the photochemical catalyst [2,19]. The active sites of photo-catalysts can be increased by increasing surface area and crystalline structure; these in turn increase the effectiveness of photo-catalytic reactions by separating electron-hole pairs [19].

### Antioxidant activities

#### DPPH radical scavenging

The results of DPPH radical scavenging assay for different concentrations of CuO nanoparticles are shown in Table 2 in the form of  $IC_{50}$  values. The highest  $IC_{50}$  value ( $84 \pm 0.32 \mu\text{g/ml}$ ) was seen at a concentration of  $1000 \mu\text{g/mL}$ , while the lowest  $IC_{50}$  value ( $40 \pm 0.23 \mu\text{g/ml}$ ) was obtained at a concentration of  $60 \mu\text{g/mL}$ . Hence it is evident that the DPPH free radical scavenging

increased with increasing concentration of the CuO nanoparticles. At  $1000 \mu\text{g/mL}$ , the CuO nanoparticles showed significant DPPH radical scavenging activity which was comparable to that of BHT having  $IC_{50}$  value of  $68 \pm 0.29 \mu\text{g/ml}$ . This indicates that the synthesized CuO nanoparticles possess high antioxidant activity in terms of scavenging DPPH free radicals.

#### Total phenolic contents (TPC)

High percentage of total phenolic contents ( $0.86 \pm 0.08 \text{ mg/100g}$  as GAE) was noticed in  $1000 \mu\text{g}$  of the methanol concentrate, while minimum total phenolic contents ( $19.7 \pm 0.21 \text{ mg/100 g GAE}$ ) value was observed in  $60 \mu\text{g}$  of methanol concentrate. These results are shown in Table 2. The TPC activity of the nanoparticles increased with increasing concentration.

#### Antioxidant activity via inhibition of linoleic acid oxidation

The results of antioxidant activity of different concentrations of CuO nanoparticles determined using the percentage inhibition of linoleic acid oxidation are shown in Table 2.

The percentage inhibition of linoleic acid peroxidation were  $17 \pm 0.23$ ,  $25 \pm 0.19$ ,  $37 \pm 0.15$ ,  $42 \pm 0.17$  and  $58 \pm 0.21$  for 60, 125, 250, 500 and 1000  $\mu\text{g}$  of CuO nanoparticles, respectively. Maximum inhibition was  $58 \pm 0.21$  % (for 1000  $\mu\text{g}$  of CuO nanoparticles), while the minimum percentage inhibition ( $17 \pm 0.23$  %) was recorded for 60  $\mu\text{g}$  of the nanoparticles. Linoleic oxidation was significantly inhibited by the CuO nanoparticles at all the levels tested, and the percentage inhibition was comparable to that of BHT which produced  $61 \pm 0.19$  % inhibition.

### FRAP

In the FRAP assay, the maximum antioxidant activity of  $9.10 \pm 0.21$  TE/mL was produced by 1000  $\mu\text{g}$  of the CuO nanoparticles while the minimum antioxidant activity ( $0.65 \pm 0.01$  TE/mL) was observed with 60  $\mu\text{g}$  of CuO nanoparticles. FRAP results for 1000, 500, 250, 125 and 60  $\mu\text{g}$  of CuO nanoparticles were 9.10, 4.57, 2.98, 1.90, and 0.65 g/100g TE/mL, respectively. These results are shown in Table 2.

### Total antioxidant activity (TAA)

The absorbance values obtained in TAA assay were  $0.6920 \pm 0.05$ ,  $0.3730 \pm 0.04$ ,  $0.1897 \pm 0.04$ ,  $0.1197 \pm 0.01$  and  $0.1049 \pm 0.02$  for 1000, 500, 250, 125 and 60  $\mu\text{g}$  of CuO nanoparticles, respectively. The corresponding absorbance values for standard BHT ranged from  $0.68 \pm 0.04$  to  $0.1 \pm 0.01$  (Figure 8). Thus the TAA of the nanoparticles were in close conformity with that of BHT.

### Antibacterial activity

The results of antimicrobial activity of the CuO nanoparticles are depicted in Table 3. There was no antimicrobial activity in the water used as negative control. The CuO nanoparticle at 5mg showed effective antimicrobial activity against *S. aureus*, *Klebsiella* and *B. subtilis*, with zones of inhibition (ZOI) of  $10 \pm 0.11$  mm,  $14 \pm 0.05$  mm and  $15 \pm 0.11$  mm, respectively.

**Table 2:** Antioxidant activity of the synthesized CuO nanoparticles

Sr No.	Concentration ( $\mu\text{g}$ )	DPPH IC <sub>50</sub> ( $\mu\text{g}/\text{ml}$ )	FRAP ( $\mu\text{M}/\text{mL}$ as TE)	TPC (mg/100g as GAE)	%Inhibition of Linoleic acid oxidation
1	60	$40 \pm 0.23$	$0.65 \pm 0.01$	$0.86 \pm 0.08$	$17 \pm 0.23$
2	125	$52 \pm 0.30$	$1.90 \pm 0.12$	$1.82 \pm 0.11$	$25 \pm 0.19$
3	250	$68 \pm 0.29$	$2.98 \pm 0.09$	$4.98 \pm 0.15$	$37 \pm 0.15$
4	500	$76 \pm 0.33$	$4.57 \pm 0.19$	$10.1 \pm 0.25$	$42 \pm 0.17$
5	1000	$84 \pm 0.32$	$9.10 \pm 0.21$	$19.7 \pm 0.21$	$58 \pm 0.21$
6	BHT	$68 \pm 0.29$	-	-	$61 \pm 0.19$

Values are mean  $\pm$  SD 9N = 30

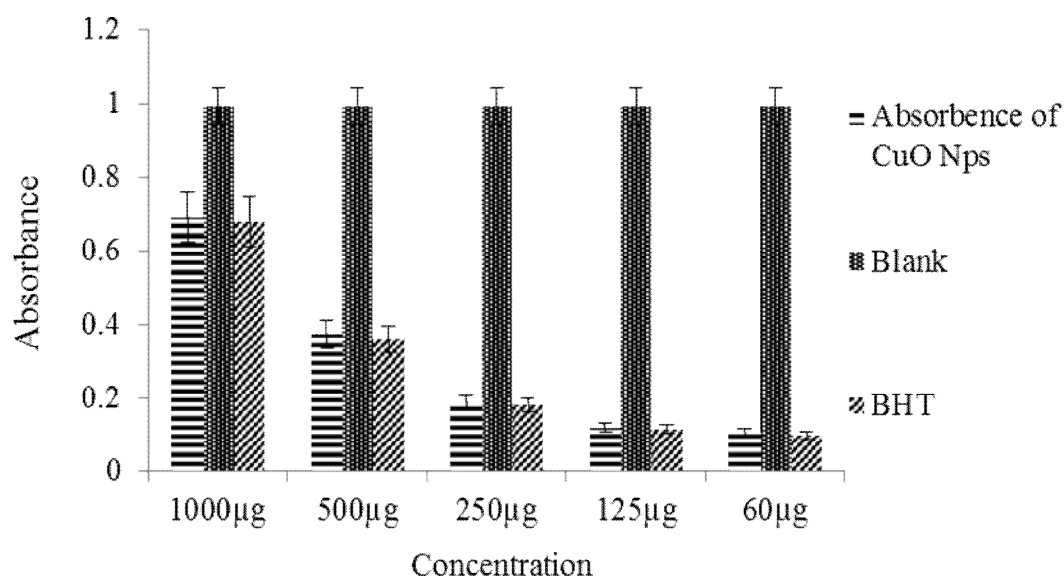


**Figure 8:** Total antioxidant activity of CuO nanoparticles



**Table 3:** Zone of inhibition (mm) of CuO nanoparticles and ampicillin

Microorganism	Inhibition zone of diameter (mm)			MIC (mm)		
	Standard (1mg)	CuO Naps (5mg)	CuO Naps (3mg)	Standard (1mg)	CuO Naps (5mg)	CuO Naps (3mg)
	<i>E. coli</i>	10±0.09	7±0.08	6±0.04	0.1	2
<i>S. aureus</i>	12±0.05	10±0.11	6±0.09	0.08	1.12	2.0
<i>Klebsiella</i>	8±0.05	14±0.05	12±0.04	0.12	0.08	0.11
<i>B. subtilis</i>	12±0.09	15±0.11	14±0.07	0.07	0.05	0.06

CuONps = CuO nanoparticles, MIC = minimum inhibition concentration, Standard = ampicillin

With 3 mg of the nanoparticles, effective antimicrobial activity was seen only for *Klebsiella* and *B. subtilis*, with ZOI values of 12±0.04 mm and 14±0.07 mm, respectively. CuO nanoparticles exhibited strong antibacterial activity with minimum inhibitory concentration (MIC) ranged from 0.05-2.0 mg/ml. Compared with the standard drug ampicillin, it was evident that 5 mg was much more effective against *Klebsiella* and *B. subtilis*. Zone of inhibition of (Zoi) of ampicillin for *Klebsiella* and *B. subtilis* were 8.00 ± 0.05 mm and 12±0.09 mm respectively. The CuO nanoparticles showed very effective broad spectrum antibacterial activity.

## DISCUSSION

CuO nanoparticles have attracted a lot of research interest because of their significant and important roles as catalyst, ceramic resistor, superconducting material, gas sensor, as well as their roles in biological fields and in the energy sector [8]. SEM results confirmed the nano range of the synthesized CuO nanoparticles. Results also confirmed their spherical shape. These findings are in agreement with those reported in previous studies [6,7,15]. Results from EDX were consistent with the SEM results, and it was evident from the EDX spectrum that the CuO nanoparticles were synthesized successfully. The major constituents of the nanoparticles were Cu (36.95 %) and O (52.09 %), and negligible impurities (S, Si, P). It was also confirmed from EDX results that the CuO nanoparticles were crystalline, based on their strong, intense, narrow width and sharp peaks in the EDX spectrum. The EDX results in the present study are similar to previously published data [16]. Sharp peaks of the synthesized CuO nanoparticles also appeared in the XRD spectrum, which confirmed their crystalline nature and supported the EDX results. The XRD results were in close agreement with previously published data, but with slight differences [2,3].

The energy band gap result for the synthesized CuO nanoparticles (3.378 eV) in the current study was slightly higher when compared with

previously reported data. This is likely due to the effect of some amorphous and nanostructured impurities (S, Si, P) that were present in the CuO nanoparticles; these were responsible for the increased energy band gap [17]. The nature of the synthesized CuO nanoparticles as photo-catalyst was evident from the disintegration phenomenon in which the organic nature commercial grade Acid Black 210 dye was degraded by the nanoparticles. The CuO nanoparticles completely disintegrated the Acid Black 210 dye into CO<sub>2</sub> and H<sub>2</sub>O within one hour. The high disintegrative capacity of the CuO nanoparticles is due to their crystalline nature, because studies have shown that the higher the crystalline nature, the higher the disintegrative ability and the disintegration rate [2,19].

Different amounts of the synthesized CuO nanoparticles were investigated for antioxidant potential in terms of total antioxidant (TAA). The results revealed concentration-dependent antioxidant effects, with 1000 µg producing the most potent antioxidant effects. Similar concentration-dependent antioxidant properties have been reported previously [3]. Interestingly, 1000 µg of CuO nanoparticles produced antioxidant effects similar and comparable to that of the standard antioxidant BHT with respect to percentage inhibition of linoleic acid peroxidation, DPPH assay and total antioxidant assay. These results are in close agreement with previously reported data [8].

The CuO nanoparticles at 5 mg and 1 mg, produced higher antimicrobial effects than the standard drug Ampicillin in the inhibition of growth of *Klebsiella*, *Bacillus subtilis*, *Escherichia coli* and *Staphylococcus aureus*.

This superior antimicrobial activity was due to the fact that the copper ions released from CuO nanoparticles permeated the bacterial cell membrane and destroyed the structure of the cell membrane by attaching to the negatively-charged cell wall [1,2]. Copper ions are involved in cross-linkage of nucleic acid strands by binding them with DNA molecule of bacteria. This results in a disordered helical structure of DNA

molecule which causes denaturation of proteins and some other biochemical processes in the cell, leading to complete destruction of the bacterial cell [3]. Factors which affect the sensitivity of bacteria to cupric oxide nanoparticle are size of particles, temperature of synthesis of the nanoparticles, structure of bacterial cell wall, and degree of contact of the nanoparticles with bacteria [6].

## CONCLUSION

The results obtained in this study show that the synthesized CuO nanoparticles possess potent and desirable biological activities. These include good photo-catalytic, antimicrobial and antioxidant activities. In future, this green method of synthesizing CuO nanoparticles could also be extended to the fabrication of other industrially important metal oxides.

## DECLARATIONS

### Acknowledgement

This work was supported by the Department of Chemistry, School of Science, University of Management and Technology, Lahore, Pakistan.

### Conflict of Interest

No conflict of interest associated with this work.

### Contribution of Authors

The authors declare that this work was done by the authors named in this article and all liabilities pertaining to claims relating to the content of this article will be borne by them.

### Open Access

This is an Open Access article that uses a funding model which does not charge readers or their institutions for access and distributed under the terms of the Creative Commons Attribution License (<http://creativecommons.org/licenses/by/4.0>) and the Budapest Open Access Initiative (<http://www.budapestopenaccessinitiative.org/read>), which permit unrestricted use, distribution, and reproduction in any medium, provided the original work is properly credited.

## REFERENCES

1. Ren G, Hu D, Cheng EW, Vargas-Reus MA, Reip P, Allaker RP. Characterization of copper oxide nano particles for antimicrobial applications. *Int J Antimicrob Agents* 2009; 33(6): 587-590.
2. Sankar R, Manikandan P, Malarvizhi V, Fathima T, Shivashangari KS, Ravikumar V. Green synthesis of colloidal copper oxide nanoparticles using *Carica papaya* and its application in photocatalytic dye degradation. *Spectrochim Acta Mol Biomol Spectrosc* 2014; 121: 746-750.
3. Yallappa S, Manjanna J, Sindhe MA, Satyanarayan ND, Pramod SN, Nagaraja K. Microwave assisted rapid synthesis and biological evaluation of stable copper nanoparticles using *T. arjuna* bark extract. *Spectrochim Acta Mol Biomol Spectrosc* 2013; 110: 108-115.
4. Kwak K, Chongyoun K. Viscosity and thermal conductivity of copper oxide nanofluid dispersed in ethylene glycol. *Korea-Aust Rheol j* 2005; 17(2): 35-40.
5. Stoimenov PK, Rosalyn L, Klinger, George LM, Kenneth JK. Metal oxide nanoparticles as bactericidal agents. *Langmuir* 2002; 18(17): 6679-6686.
6. Das SK, Khan MMR, Guhab AK, Naskar N. Bioinspired fabrication of silver nanoparticles on nanostructured silica: characterization and application as a highly efficient hydrogenation catalyst. *Green Chem* 2013; 15: 2548-2557.
7. Iravani S. Green synthesis of metal nanoparticles using plants. *Green Chem* 2011; 13 (10): 2638-2650.
8. Sankar R, Karthik A, Prabu A, Karthik S, Shivashangari KS, Ravikumar V. *Origanum vulgare* mediated biosynthesis of silver nanoparticles for its antibacterial and anticancer activity. *Colloids and Surfaces B: Biointerfaces* 2013; 108: 80-84.
9. Khan SA, Rasool N, Riaz M, Nadeem R, Rashid U, Rizwan K, Zubair M, Bukhari IH, Gulzar T. Evaluation of Antioxidant and Cytotoxicity Studies of *Clerodendrum inerme*. *Asian J Chem* 2013; 13: 7457-7462.
10. Prieto P, Pineda M, Aguilar M. Spectrophotometric quantitation of antioxidant capacity through the formation of a phosphomolybdenum complex: specific application to the determination of vitamin E. *Anal Biochem* 1999; 269: 337-341.
11. Benzie IEF, Strain JJ. The ferric reducing ability of plasma (FRAP) as a measure of antioxidant power: the FRAP assay. *Anal. Biochem* 1996; 239: 70-76.
12. Makkar HPS, Bluemmel M, Borowy NK, Becker K. Gravimetric determination of tannins and their correlations with chemical and protein precipitation methods. *J Sci Food Agr* 1993; 61: 161-165.
13. Valentao P, Fernandes E, Carvalho F, Andrade PB, Seabra RM, Bastos ML. Antioxidative properties of cardoon (*Cynara cardunculus* L.) infusion against superoxide radical, hydroxyl radical, and hypochlorous acid. *J Agr Food Chem* 2002; 50: 4989-4993.
14. Khan SA, Shahid S, Jameel M, Ahmad A. In vitro Antibacterial, Antifungal and GC-MS Analysis of seeds of Mustard Brown. *Int J Pharma Chem* 2016; 6(4): 107-115.
15. Saif S, Tahir A, Asim T, Chen Y. Plant mediated green synthesis of CuO nanoparticles: comparison of toxicity

- of engineered and plant mediated CuO nanoparticles towards Daphnia magna. Nanoma 2016; 6(205): 1-15.*
16. Ren G, Hu D, Cheng EW, Vargas-Reus MA, Reip P, Allaker RP. Characterization of copper oxide nanoparticles for antimicrobial applications. *Int J Antimi Age* 2009; 33(6): 587-590.
  17. Rafea MA, Roushdy N. Determination of the optical band gap for amorphous and nanocrystalline copper oxide thin films prepared by SILAR technique. *Journal of Physics D: App Phys* 2008; 42(1): 1-6.
  18. Lai CW, Juan JC, K WB, Hamid SBA. An overview: recent development of Titanium Oxide nanotubes as photocatalyst for dye degradation. *Int J Photo* 2014; 2014: 1-14.
  19. Dashamiri S, Ghaedi M, Dashtian K, Rahimi MR, Goudarzi A, Jannesar R. Ultrasonic enhancement of the simultaneous removal of quaternary toxic organic dyes by CuO nanoparticles loaded on activated carbon: central composite design, kinetic and isotherm study. *Ultra sonochem* 2016; 31(31): 546-557.